9

Theory, Algorithms and Applications for Solar Panel MPP Tracking

Petru Lucian Milea[1], Adrian Zafiu[2], Orest Oltu[1] and Monica Dascalu[1]
[1]"Politehnica" University of Bucharest,
[2]Romanian Academy Research Institute for Artificial Intelligence
Romania

1. Introduction

The photovoltaic panel is a power source whose parameters depend on some external factors like incident light angle, shading, ambient temperature etc. Some of these factors are unpredictable and, for this reason, so is the evolution of cell parameters. The most known parameters of the photovoltaic panel are the open circuit voltage (V_{oc}) and short circuit current (I_{sc}). These values define the points where the I(V) graph curve of the panel intersects the two axes (I and V), like in Fig. 1.

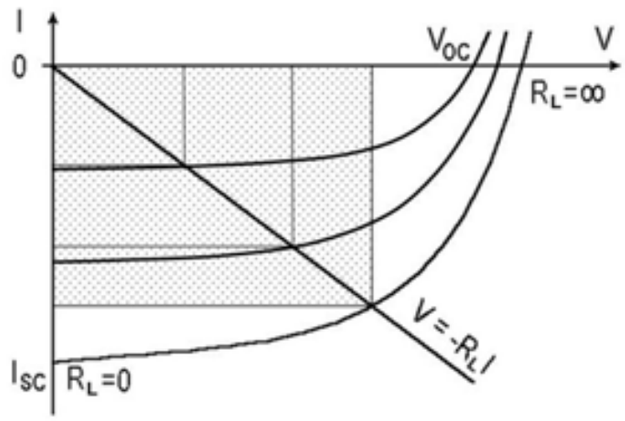

Fig. 1. Some *I(V)* characteristics of a photovoltaic panel under different work conditions

Every point on the I(V) curve has specific values of V_i and I_i, defining the power as $P_i = V_i \cdot I_i$. For a specific I(V) curve there is only one point corresponding to the maximum power. This is named maximum power point or MPP. For any power source it is always good to supply electrical consumers at this value or close to it. For a specific resistive load, R_L, the $I_{RL}(V)$ load characteristic is a line given by the equation $I_{RL} = -I = V/R_L$. This line intersects the panel characteristic in a point which is near or far from MPP (Fig. 1.). According to this position, the power transferred to the load can be only a fraction of the power that panel can supply at MPP. To correct this unbalance and prevent the associated lose of usefully power, some methods, generically named MPPT (Maximum Power Point Tracking) are used.

MPPT methods are designed to tune the electrical current to the value corresponding to MPP. This means, in other words, to adapt the impedance of the consumers to the optimal impedance for the best power transfer. For this reason, we named the resulted circuits as "impedance adapters". For the studied case, characterized by the almost permanent modification of the I(V) curve, the MPP varies almost at every moment, therefore the power maximization process needs a dynamic impedance adaptor.
In the studied scientific literature, we found some algorithms which are purposed to implement this function, but the adaptation speed may be a problem for some of them (Yang et al., 2008). We start this study in order to find solutions for simple, fast and accurate (efficient) MPPT. For this purpose, we propose two computational algorithms and a impedance adjustment method which use DC/DC converters. The tracking method was designed to be able to track the MPP for an unknown type of solar panel (viewed as a black box) and external conditions (irradiance and temperature). The algorithms were simulated with a dedicated application and the results were compared with other algorithm results and also with some experimental data.

2. The mathematical model

We propose a mathematical model to estimate the maximal power point of a panel, starting from the simplest model of a photovoltaic cell.
The photovoltaic cell *I(V)* characteristic, presented in Fig 2, is given by a equation derived from the Shockley diode equation:

$$I(V) = I_0\left(e^{V/(a\cdot V_T)} - 1\right) - I_L\,, \tag{1}$$

where, I_0 is the reverse saturation current, V_T is the thermal voltage ($V_T=kT/q$, with $q=1.602x10^{-19}C$ the electron charge, T – jonction temperature and $k=1.381x10^{-23}J/K$ is Boltzmann constant), a is known as the diode ideality factor (for silicon diodes a is between 1 and 2) and I_L is cell illumination current.

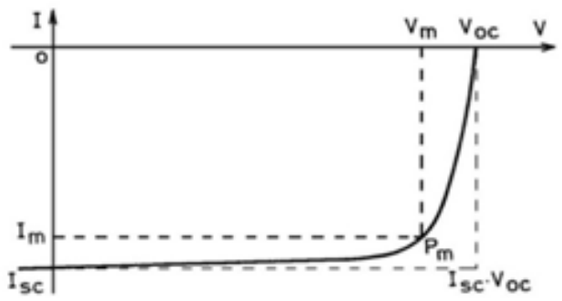

Fig. 2. The parameters of I-V cell illumination characteristic

The maximal power point, P_m, corresponds to the point where the power transferred from the panel/cell to the consumer is maximal. The ratio of P_m and the product $I_{SC} \cdot V_{OC}$ (the dotted areas) define the fill factor, *FF*, which represents a measure of the resistive losses of the device.
For the cell illumination current we choose to use a formula based on datasheet parameters of the cell or panel (Chenni et al., 2007):

$$I_L = \left(I_{Lref} + \alpha\left(T - T_{ref}\right)\right)G/G_{ref}\ , \tag{2}$$

where: G_{ref}=1kW/m² represents the irradiation at *AM1,5*, T_{ref}=25⁰C, I_{Lref}*(A)* has value I_L at G_{ref} and T_{ref}, *a(A/K)* is the temperature coefficient at short circuit.
The reverse saturation current, I_0, is given by the relation:

$$I_0 = DT^3 e^{-q\varepsilon_g/akT} = DT^3 e^{-\varepsilon_g/aV_T} \tag{3}$$

For the ideal photovoltaic cell (without resistive losses – Fig. 3.a) we have equation:

$$I_1 = I_0\left(e^{\frac{V_1}{aV_T}} - 1\right) - I_L = I_{0ref}\left(\frac{T}{T_{ref}}\right)^3 e^{\frac{\varepsilon_g}{aV_T}\left(\frac{T}{T_{ref}}-1\right)}\left(e^{\frac{V_1}{aV_T}} - 1\right) - \frac{G}{G_{ref}}\left(I_{Lref} + \alpha\left(T - T_{ref}\right)\right) \tag{4}$$

The real photovoltaic cell contains also energy dissipation elements. For the approximate model, presented in figure 3.b, the relation *I(V)* becomes:

$$I_2 = I_0\left(e^{\frac{V_2 - I_2 R_s}{aV_T}} - 1\right) - I_L - \frac{V_2 - I_2 R_s}{R_p} \tag{5}$$

In order to adapt the model for a panel, we take into account that this is formed by a matrix of NS x NP cells (Fig. 4.). The cell parameters are scaled as follows: $I_L^P = N_p I$, $I_0^P = N_p I_0$, $V_3 = N_s V_2$, $I_3 = N_p I_2$, $I_3 = N_p I_2$, $R_s^P = R_s \frac{N_s}{N_p}$, $R_p^P = R_p \frac{N_s}{N_p}$.

We obtain the global *I(V)* equation of the panel:

$$I_3 = I_0^P\left(e^{\frac{V_3 - I_3 R_s^P}{aN_s V_T}} - 1\right) - I_L^P - \frac{V_3 - I_3 R_s^P}{R_p^P} \tag{6}$$

The MPP condition for transferred power is defined as follows:

$$\left.\frac{dP}{dV}\right|_{MPP} = \left.\frac{d(I_{RL}\cdot V)}{dV}\right|_{MPP} = \left.\frac{d(-I\cdot V)}{dV}\right|_{MPP} = -V\left.\frac{dI}{dV}\right|_{MPP} - I\left.\frac{dV}{dV}\right|_{MPP} = 0 \tag{7}$$

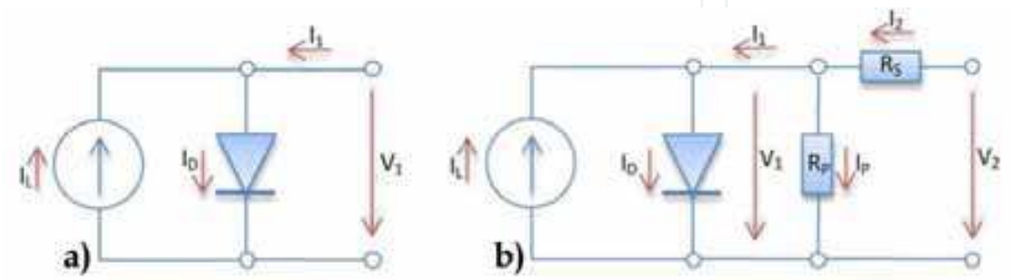

Fig. 3. Two equivalent circuits of PV cell: a) an ideal circuit, b) an equivalent circuit with serial and parallel resistive loses

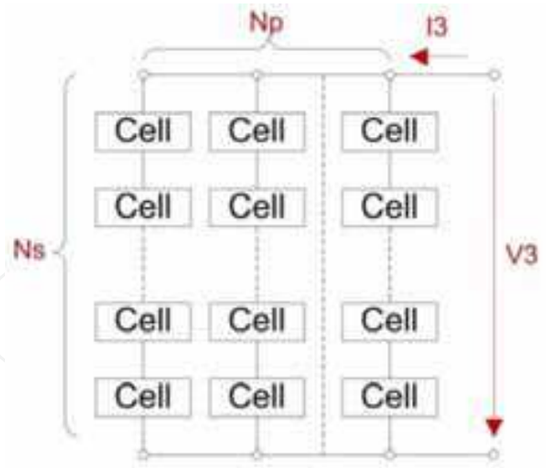

Fig. 4. A photovoltaic panel, as a matrix of N_S x N_P cells

Denoting with R_X the value of resistive load at MPP, R_X=-V_m/I_m, we obtain:

$$\left.\frac{dI}{dV}\right|_{MPP} = -\frac{I}{V} = \frac{1}{R_X} \tag{8}$$

For the studied cases, from the relation (8), we obtain:

$$R_{x1} = aV_T \,/\, (I_0 e^{V_1 / aV_T}) \tag{9}$$

$$R_{X2} = R_S + 1/(1/R_p + 1/R_{X1}) \tag{10}$$

$$R_{X3} = R_{X2} N_S / N_P \tag{11}$$

which can be replaced in the following equation, to obtain the PV cell/panel MPP current:

$$I = -\frac{V}{R_X} \tag{12}$$

The equation (12) is a nonlinear implicit equation and has to be solved numerically. For the ideal model of a PV cell, the equation to be solved is:

$$\left(\frac{V_1}{aV_T} + 1\right) e^{\frac{V_1}{aV_T}} = \frac{\frac{G}{G_{ref}}\left(I_{Lref} + \alpha\left(T - T_{ref}\right)\right)}{I_{0ref}\left(\frac{T}{T_{ref}}\right)^3 e^{\frac{\varepsilon_g}{aV_T}\left(\frac{T}{T_{ref}} - 1\right)}} \tag{13}$$

Also we solved this equation graphically (Fig. 5.), at the intersection of the curves *I(V)* (cell/panel characteristic) and $I_m(V)$, where we denoted I_m=-V/R_X, under specific conditions. From the graphics we observed the relatively constant value of *FF*, for relatively high variations of *G* and *T*. A numerical solution can be also obtained following this principle.

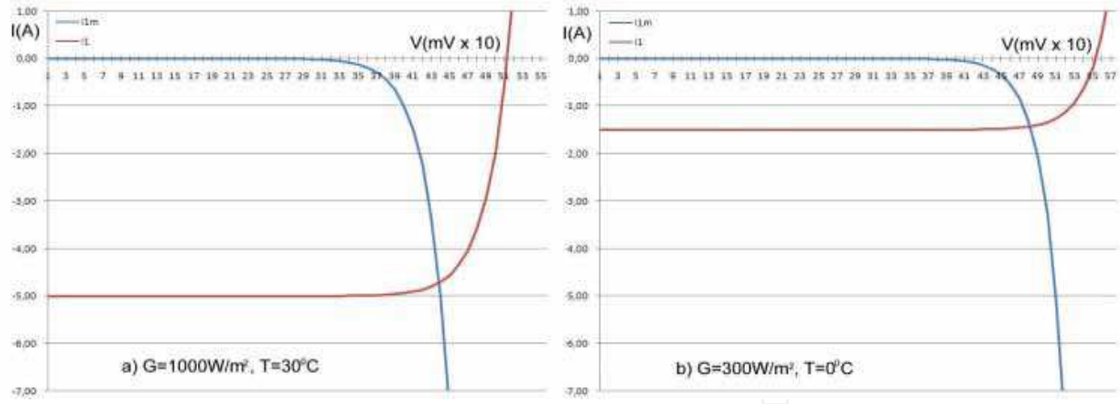

Fig. 5. The graphic solution of the MPP equation for two datasets of G and T

In practical applications, the MPP tracking is made in an iterative manner, similar with numerical solution, trough iterative adjustment of the charge's impedance to the necessary value, with the aid of a DC/DC converter (boost, buck or buck–boost converter). For this type of application we implement two types of algorithms which are presented in section 4.

3. MPPT advantages evaluation, based on proposed model

To assess the benefits of using a MPPT circuit, we consider that it is based on a buck-boost converter. We'll make a comparative analysis of the energetic transfer from photovoltaic panel to a battery by using a direct load circuit and a MPPT circuit respectively.
In this evaluation we will estimate the energetic transfer in a summer day, when the panel temperature varies between T_0=290K at sunrise and T_{max}=330K at middle day, when the Sun is at meridian. To reduce the computational complexity we suppose that the panel tracks the direction to the Sun, so the direct irradiation is always upright on the panel.
In this simplified hypothesis we suppose that global radiation *AM1* has value G_0=1000W/m² and the global radiation during all day is inverse with the optical path (air mass) throw atmosphere (m_r).

$$G = \frac{G_0}{m_r}, \tag{9}$$

where m_r is given by (Milea, 2010):

$$m_r = 531 \cdot \left(\sqrt{1/265{,}25 + \cos^2(z)} - \cos(z) \right) \tag{10}$$

To estimate the panel temperature, we used a simplified formula, considering that it is directly dependent with the Sun's position. Under this aproximative model, for a cloudless summer day, the diurnal variation of the panel temperature will be (Milea, 2010):

$$T = T_0 + \frac{\Delta T}{m_r}, \tag{11}$$

where T=290K and ΔT=40K.
For a panel with N_S x N_P cells, based on the ideal model, the open circuit voltage formula is:

$$V_{OC} = a \cdot V_T \cdot N_S \cdot \ln\left(1 + \frac{I_L}{I_0}\right) \tag{12}$$

The short circuit current is:

$$I_{SC} = N_P \cdot I_L = N_P \frac{G}{G_{ref}}\left(I_{Lref} + \alpha\left(T - T_{ref}\right)\right) \tag{13}$$

To model a solar panel for off-grid application with a DC bus of 12V, under reference conditions, we choose N_S=44 taking into account that V_{OCcref}=0,51V, for a single cell. The obtained open voltage of the panel is V_{OCref}=22,64V, which is a common value for such applications.

For the mentioned parameters, we determined the values of V_{OC}, I_{SC} and P_{MAX} for G and T values corresponding to different hours of a cloudless summer day. The results are plotted in Fig. 6.

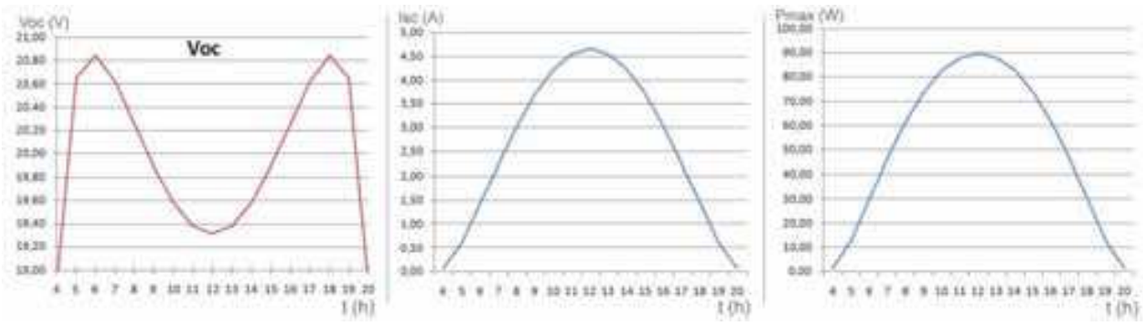

Fig. 6. V_{OC}, I_{SC} and P_{MAX} curves at different hours of a cloudless summer day

Note that the voltage is always greater than 19V, while the current and maximum reference power curves have a gait similar to that of the optical path.

If direct charging of accumulator batteries, since the panel voltage is significantly higher than the battery's one (Milea, 2010), we can assume with a very good approximation that the battery will charge at the panel's short-circuit current:

$$P_{DIR} = V_{bat} \cdot I_{SC} = V_{bat} \cdot N_P \cdot \frac{G}{G_{ref}}\left(I_{Lref} + \alpha\left(T - T_{ref}\right)\right) \tag{13}$$

From (9) şi (13), because the irradiance references, G_0 and G_{ref} , are identical, we obtain:

$$P_{DIR} = \frac{V_{bat} \cdot N_P}{m_r}\left(I_{Lref} + \alpha\left(T_0 + \frac{\Delta T}{m_r} - T_{ref}\right)\right) \tag{14}$$

For the cosine function of the zenith angle of a summer day, in Bucharest, Romania, we used an approximated relation (Milea, 2010):

$$\cos(z) = 0,2813 + 0,6488 \cdot \cos(0,2618 \cdot t + 2,8117)\ , \tag{15}$$

where t is the legal time of Bucharest, expressed in hours.

If the battery is charged using a MPPT charger, approximating *FF=0.8* as constant throughout the day (Fig. 5.), we get:

$$P_{MPP} = V_m \cdot I_m = FF \cdot V_{OC} \cdot N_P \cdot I_{SC} \cdot \eta = FF \cdot V_{OC} \cdot N_P \cdot \eta \cdot \frac{G}{G_{ref}} \left(I_{Lref} + \alpha \left(T - T_{ref} \right) \right), \quad (16)$$

where $\eta = 0,95$ is the efficiency of the MPPT charger.
From (9) and (16), we obtain:

$$P_{MPP} = \frac{FF \cdot V_{OC} \cdot N_P \cdot \eta}{m_r} \left(I_{Lref} + \alpha \left(T_0 + \frac{\Delta T}{m_r} - T_{ref} \right) \right) \quad (17)$$

The instant ratio of powers in the two cases will be:

$$\frac{P_{MPP}}{P_{DIR}} = \frac{FF \cdot V_{OC} \cdot \eta}{V_{bat}} = \frac{FF \cdot \eta \cdot a \cdot V_T \cdot N_S \cdot \ln\left(1 + \frac{I_L}{I_0} \right)}{V_{bat}} = \frac{\eta \cdot a \cdot FF \cdot N_S}{V_{bat}} V_T \cdot \ln\left(1 + \frac{I_L}{I_0} \right) \quad (18)$$

Based on these relations we calculate the powers supplied by a solar panel to the battery by direct connection (P_{DIR}), and through a MPPT charger (P_{MPP}). All calculations are made for a cloudless summer day. The two powers and their ratio are plotted in Fig. 7.

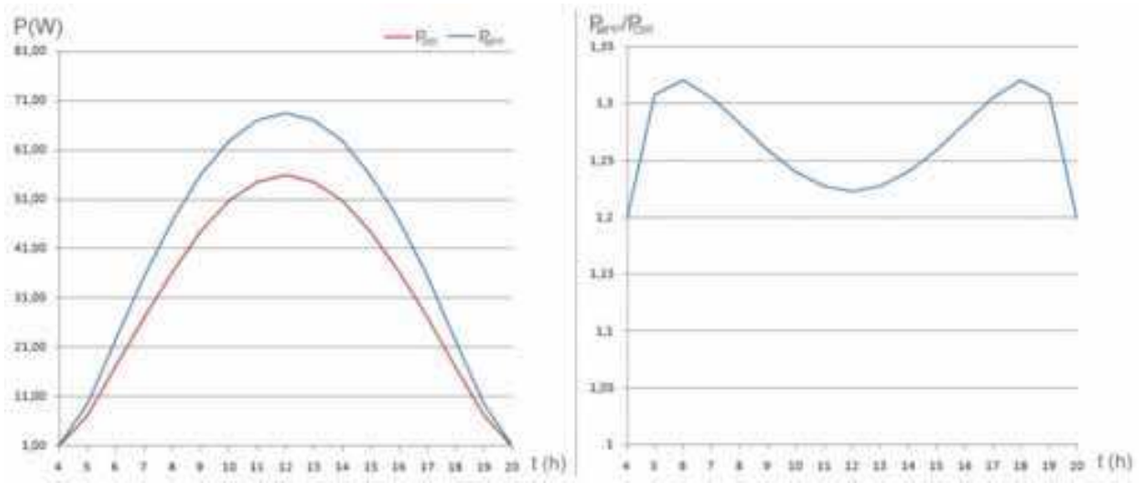

Fig. 7. Direct power and MPPT power (left) and the power ratio (right)

If we evaluate the daily average power gain of using MPPT, starting from average hourly values, we get:

$$\frac{\overline{P_{MPPs}}}{\overline{P_{DIRs}}} = 1,2 + \frac{2 \cdot \left(\frac{0,11}{2} + 0,11 + \frac{0,01}{2} + 6 \cdot 0,02 + \frac{6 \cdot 0,1}{2} \right)}{16} = 1,2 + \frac{0,59}{8} = 1,274 \quad (19)$$

So in summer, MPPT circuits provide an average increase of 27.4% transferred powers.
Making the same calculations for the winter, we get the following chart:

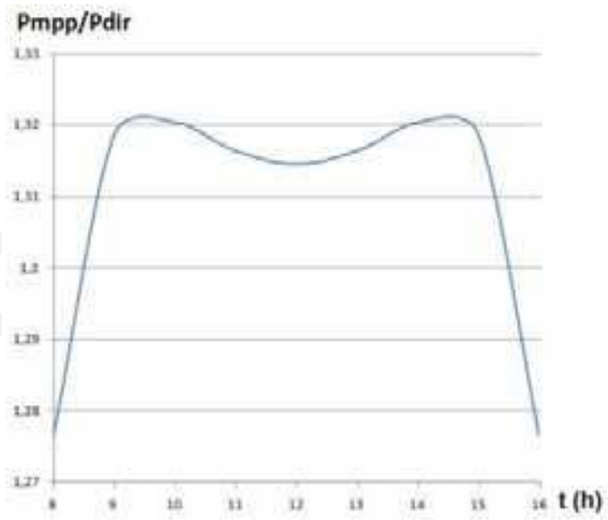

Fig. 8. Power ratio under winter conditions

If we evaluate the average MPPT power gain for winter, we get:

$$\frac{\overline{P_{MPPw}}}{\overline{P_{DIRw}}} = 1,276 + \frac{2 \cdot \left(\frac{0,04}{2} + 2 \cdot 0,04 + 2 \cdot \frac{0,003}{2} + 0,04 \right)}{8} = 1,276 + \frac{0,143}{4} = 1,312 \,, \qquad (20)$$

It follows an average power gain of 31.2%, higher than in summer.
Therefore, the minimum power gain, obtained by MPP tracking, is 27.4%.

4. Proposed MPPT algorithms

The maximum power point (MPPT) tracking algorithms use the I(V) characteristic and the P(V) characteristic. All over the world there are many studies concerning the maximum power point (MPP) tracking. The performance of various types of MPPT algorithms (Chenni et al., 2007), (Faranda et al., 2007), (Santos et al., 2006), (Hui, 2008) is always measured by precision tracking of MPP and responsiveness to changes in the power curve.
In several studies we have addressed MPP tracking algorithms (Zafiu et al., 2009) and have designed new solutions, original circuits and applications for this purpose (Milea, 2010).
To determine the MPP we used previous mathematical relationships to create the algorithms presented in this section.
The proposed MPP tracking algorithms stands upon the relation $dP/dV=0$ and involves the continuous adjustment of impedance adaption circuit (increasing or decreasing). Initially we choose two points so that $dP/dV<0$, respectively $dP/dV>0$, and the MPP is estimated to the medium value of these two points. Then, while $dP/dV>err$, the distance between points will be decreases and the MPP will take again the medium value of these points. The principle of MPP determination follows two phases. Firstly there is the measurement of three successive points (according to V) in the coordinates of I and V. Secondly, starting from these three points, the control circuit will decide the next adjustment to achive the MPP.

4.1 General presentation of the algorithms principle

This algorithm considers the values of three points (the last measured values) and Δ the distance between points. The measured value is in the middle and the other points are equidistant positioned on the left and on the right side of middle point (Fig. 9.).

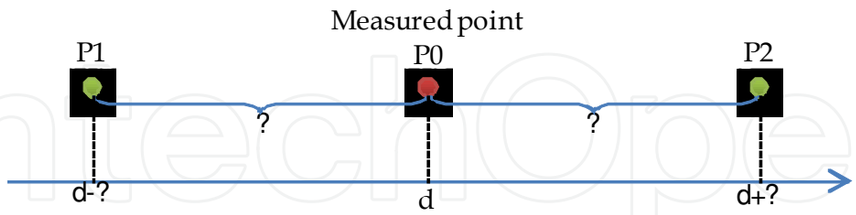

Fig. 9. Point's relative position

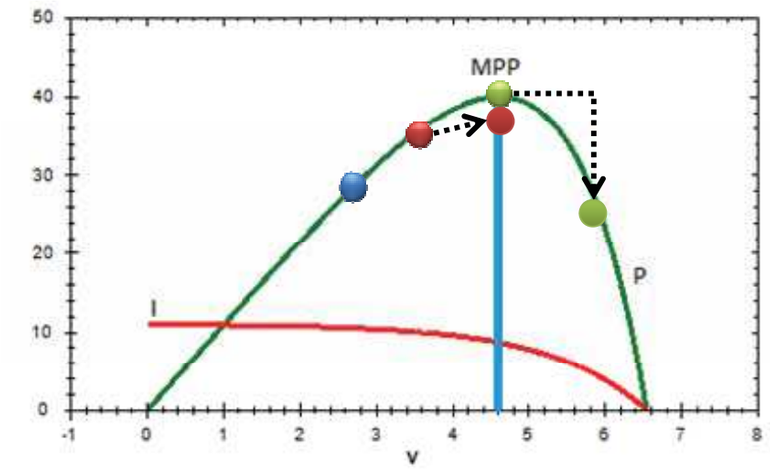

Fig. 10. Example of adjusting *d* and *Δ* so that MPP is between *d-Δ* and *d+Δ*

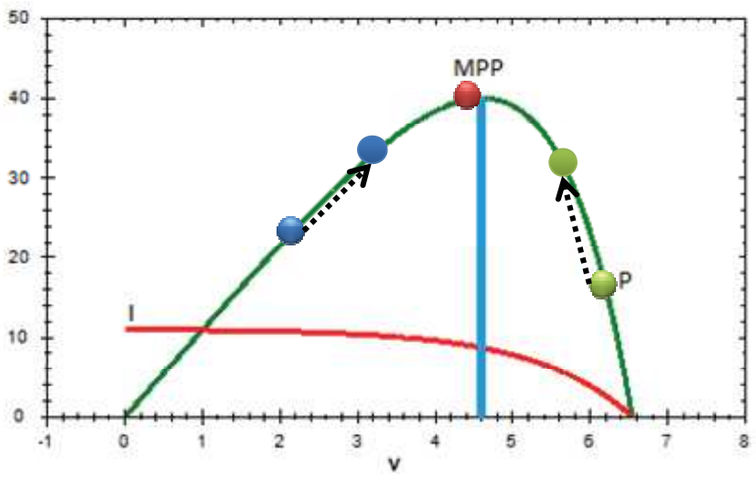

Fig. 11. Example where *Δ* is progressively reduced

It is considered that the three points are equidistant. Variable d corresponds to the value of the middle range (maximum power point value). Boundary values of the range are given by d-Δ (first point) and d+Δ (last point).
At each step of the algorithm, values of d and Δ are adjusted so that the middle point is located on top of the curve describing the power given by the photovoltaic module. If the points come to be on the same slope of the curve, distance Δ is increased so that move the middle point at the peak of the curve. If MPP was not peaked and the three points are in the pattern $P_1 < P_0$ and $P_2 < P_0$ then Δ will be reduced.
The domain of values used to represent voltage points is building using an n-bit representation. The number of bits determines the adjustment quantum and the algorithm error. The intermediate values couldn't be represented.

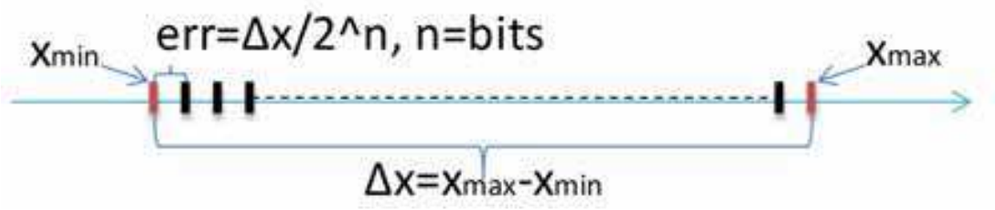

Fig. 12. The principle of building range of values using the n-bit representation

The values and errors are computed by starting from minimum and maximum values. The interval is spitted into 2^n intervals. The subinterval lentgh is $err = (x_{\max} - x_{\min}) / 2^n$. This length is also used as error value.
Following studies and tests, we designed two original algorithms to determine the maximum operating point.

4.2 Algorithm with three equidistant points

This algorithm is applied to a photovoltaic cell module in which the two cells are used as ends of range. All calculations are made with some calculation error fixed in advance.
Detailed algorithm is as follows:

- computing the point of short circuit and the range in which to find this point: as long as the voltage of the second edge is less than zero, the first edge (point) will receive the value of the second edge (point), and the second edge will receive a higher value; as long as the "distance" between the two points previously obtained is higher than the acceptable error, one of the two points will close to the other point with the average of points' values, finally achieving the short circuit point.
- compute the open circuit point and the range in which to find this point: as long as the voltage of the second point is higher than zero, the first point will receive the second point value and the second point will receive another point value; as long as the "distance" between the two points is higher than the acceptable error, the two points will approach each other with the average of points' values, thereby achieving the open circuit point;
- Determine the maximum power point as follows: d is initialized with the average of short circuit and open circuit values, Δ is initialized with the difference between d and the point of short circuit; the three points are taken to determine the MPP's and are initialized with: d-Δ to the point P_1, d to the point P_0, d+Δ to the point P_2; if the "distance" between P_1 and P_0 in addition to the "distance" between P_0 and P_2 is greater than the calculation error, are treated the following cases:

- If $P_1 < P_0$ then
  - If $P_0 < P_2$ then $d = d + \Delta$ and $\Delta = \Delta * 2$;
  - If $P_0 = P_2$ then $d = d + \Delta$ and $\Delta = \Delta * 1.5$;
  - Else $\Delta = \Delta / 2$;
- If $P_1 = P_0$ then
  - If $P_0 < P_2$ then $d = d - \Delta$ and $\Delta = \Delta * 1.5$;
  - If $P_0 = P_2$ then $\Delta = \Delta * 2$;
  - Else $d = d - \Delta$ and $\Delta = \Delta / 2$;
- Else
  - If $P_0 < P_2$ then $\Delta = \Delta * 2$;
  - If $P_0 = P_2$ then $d = d - \Delta$ and $\Delta = \Delta * 1.5$;
  - Else $d = d - \Delta$ and $\Delta = \Delta * 1.5$;

After these calculations are made the following adjustments: $d = \max\left(d, P_{sc} + err\right)$, $d = \min(d, P_{oc} - err)$, $\Delta = \min\left(\Delta, \min\left(d - P_{sc}, P_{oc} - d\right)\right)$, and points P_1 , P_2 and P_0 take the appropriate values for $d - \Delta$, $d + \Delta$, respectively d .

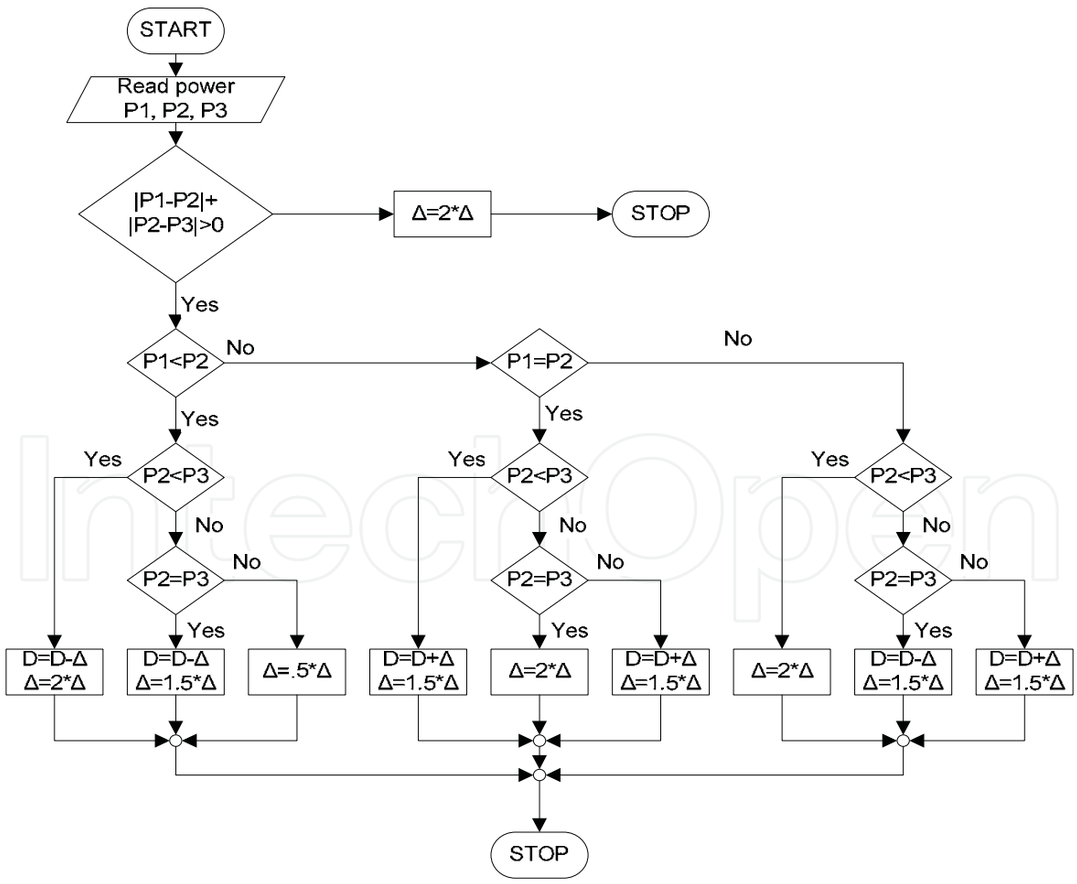

Fig. 13. The algorithm for MPP's calculation with three points

4.3 Computing MPP with a three dynamic step method

The proposed method consists in the adjustment of the pulse width which control the DC/DC converter, with dynamic step, based on the last three previous obtained successive (*I,V*) pairs. By comparing the values of that pairs, the control algorithm decides the step and direction of the next adjustment.

We consider that the first points are equidistant. Value *D* corresponds to the middle point. First point corresponds to value *D*-Δ and last point corresponds to the value *D*+Δ. At each step, the values *D* and Δ are adjusted.

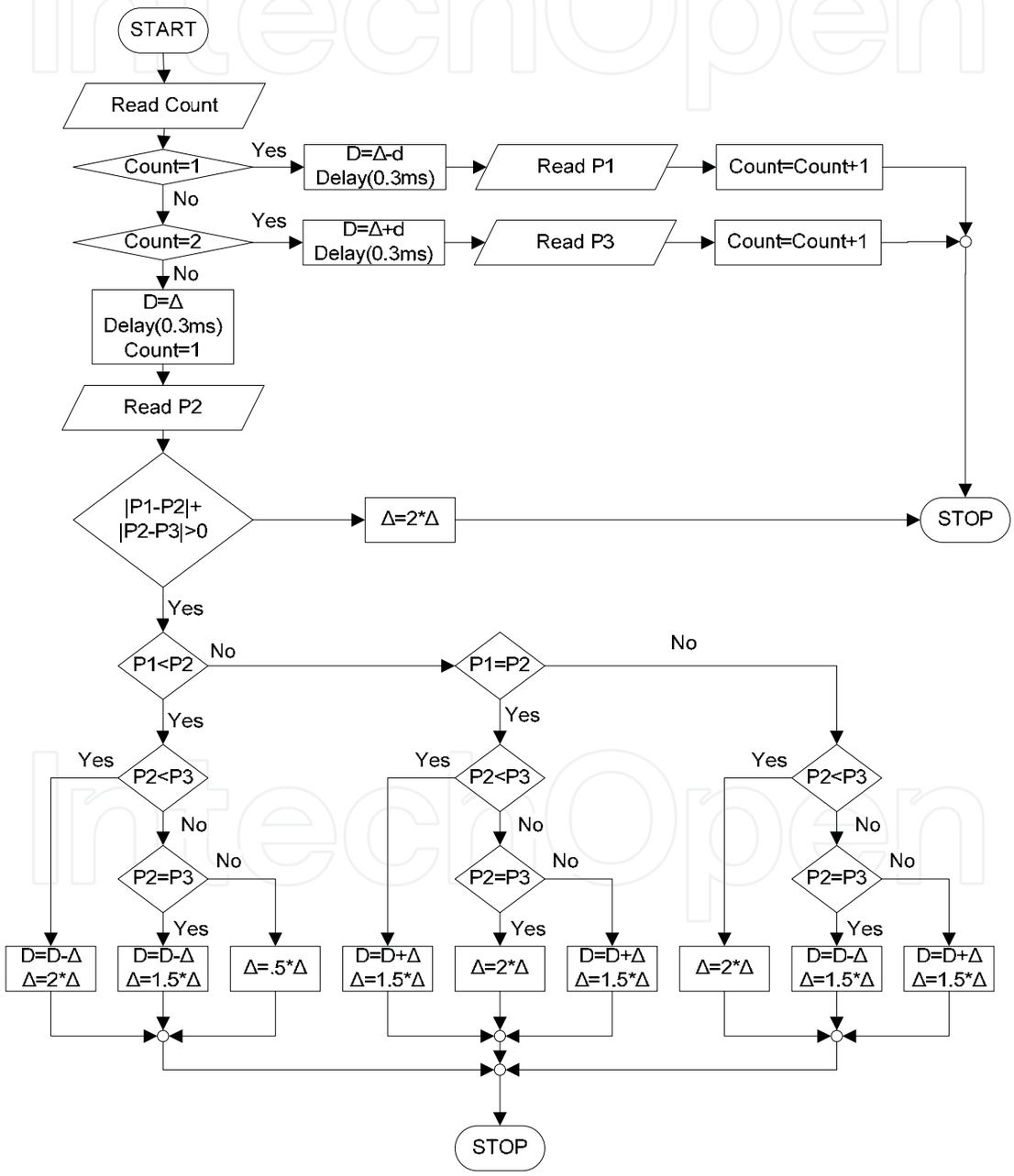

Fig. 14. The algorithm with three dynamic distanced points

5. Software application designed for mathematical model simulation and algorithm testing

For the algorithms testing we conceived and realized a software application for the modeling and simulation of cells and solar panel. Fig. 15. presents the interface for application settings, and Fig. 16. presents an example of characteristics tracing.

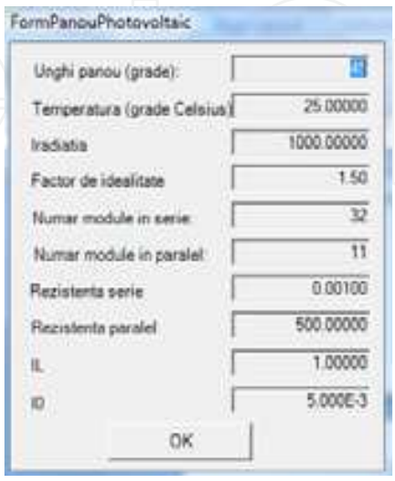

Fig. 15. Panel settings

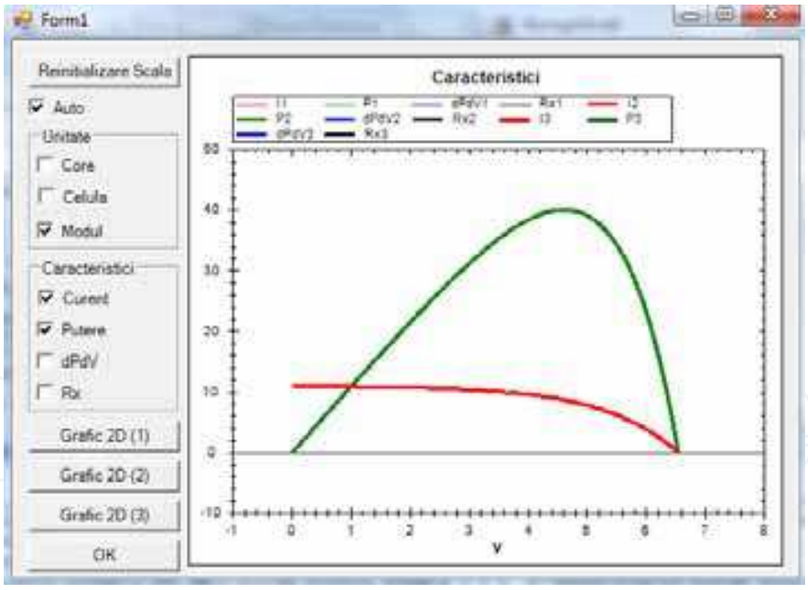

Fig. 16. The characteristic *I(V)* and *P(V)*

C# was used to design the application. The application was designed to be integrated, optionally, into an application for assessment of solar radiation intensity (Milea, 2010).
The first module represents the part in which is developed the MPP tracking algorithm for a photovoltaic cell (graphs were made using "ZedGraph library" - a set of classes written in C # for drawing 2D graphics based on arbitrary data sets; these classes provide a high degree of flexibility in that almost every aspect of the graph may be modified; ZedGraph includes a

"User Control" interface allowing editing of "drag and drop" type in the forms of Visual Studio, plus access from other languages such as C + + and Visual Basic).
Main classes implement photovoltaic cell behavior and algorithms for finding maximum power point (classes "PV" and "Algorithm").
Here you can set the angle of the panel, the temperature (if you want to see the effect of temperature on the photovoltaic cells characteristic), the solar irradiation (irradiation effect on the characteristic), the ideality factor, the number of cells connected in series, the number of cells connected in parallel, the series resistance and the parallel resistance of the equivalent circuit.
Current-voltage and power-voltage characteristics of the panel are shown in Fig. 16.
Buttons - 2D Graphics (1), 2D Graphics (2) and 2D Graphics (3) helped us to achieve the effect of temperature, irradiation and other graphs.

6. Simulations and comparative results

On the software simulation, we tested the algorithm presented in Fig. 13, on 8, 10 and 12 bits. The results are compared with the results of other algorithms and all of them are compared with the results of an ideal MPPT. The MPP tracking algorithm on 8 bits was used as reference to compare the algorithms variants. The bits number determines the discrete values that the duty cycle D can take. The newly developed algorithm uses a second variable Δ, for duty cycle adjustment, which values are dependent on the bits number, too.
The two variables can take the following values:

$$\{1/2^B, 2/2^B, 3/2^B, \ldots, 2^B - 1/2^B,\} \tag{21}$$

were B is the used number of bits.
As any tracking algorithm has no problem in estimating the maximum power if the variations are very small or non-existent (corresponding to a sunny day without clouds), the images show the behavior of our algorithm in the case of a cloudy day, where relatively high variations in G and T.
Figure 17 shows the energy output of our cell array by using our tracking algorithm on 8, 10 and 12 bits compared to the literature 8 bits method (Santos et al., 2006). The predicted duty cycle values will get the device very close to the computed theoretical maximal power point, obtaining tracking efficiencies near the maximum (100%).

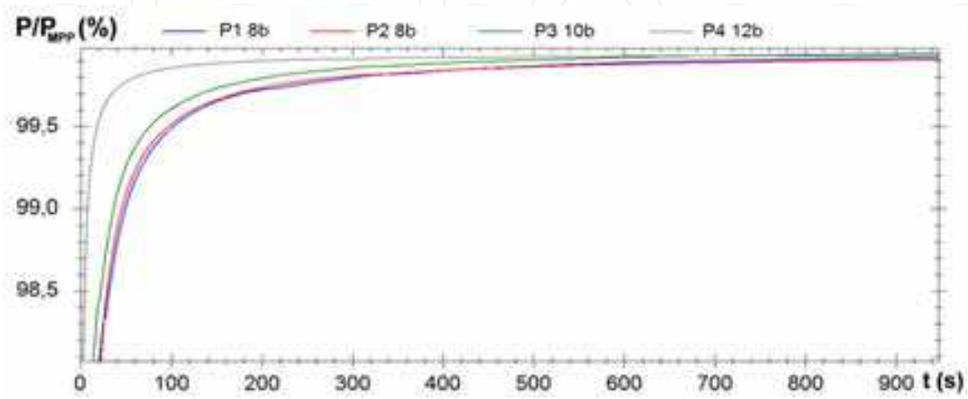

Fig. 17. The algorithm behavior: energy output
(Algorithm result for MPP calculation using *dP/dV=0* relation)

There is a small loss in energy in our algorithm for the first ~20ms until it tracks the correct values. This difference is only felt once at the algorithm's startup and is recuperated very rapidly (in ~2 seconds our algorithm becomes more efficient: 99,94% at 8 bits, 99,98% at 10 bits, while literature algorithm (Santos et al., 2006) is at 99,935%).
Fig. 18.a) shows the power output of our cell array by using our tracking algorithm on 8, 10 and 12 bits compared to the (Santos et al., 2006) method on 8 bits and Fig. 18.b) shows a detail of the power tracking behavior.

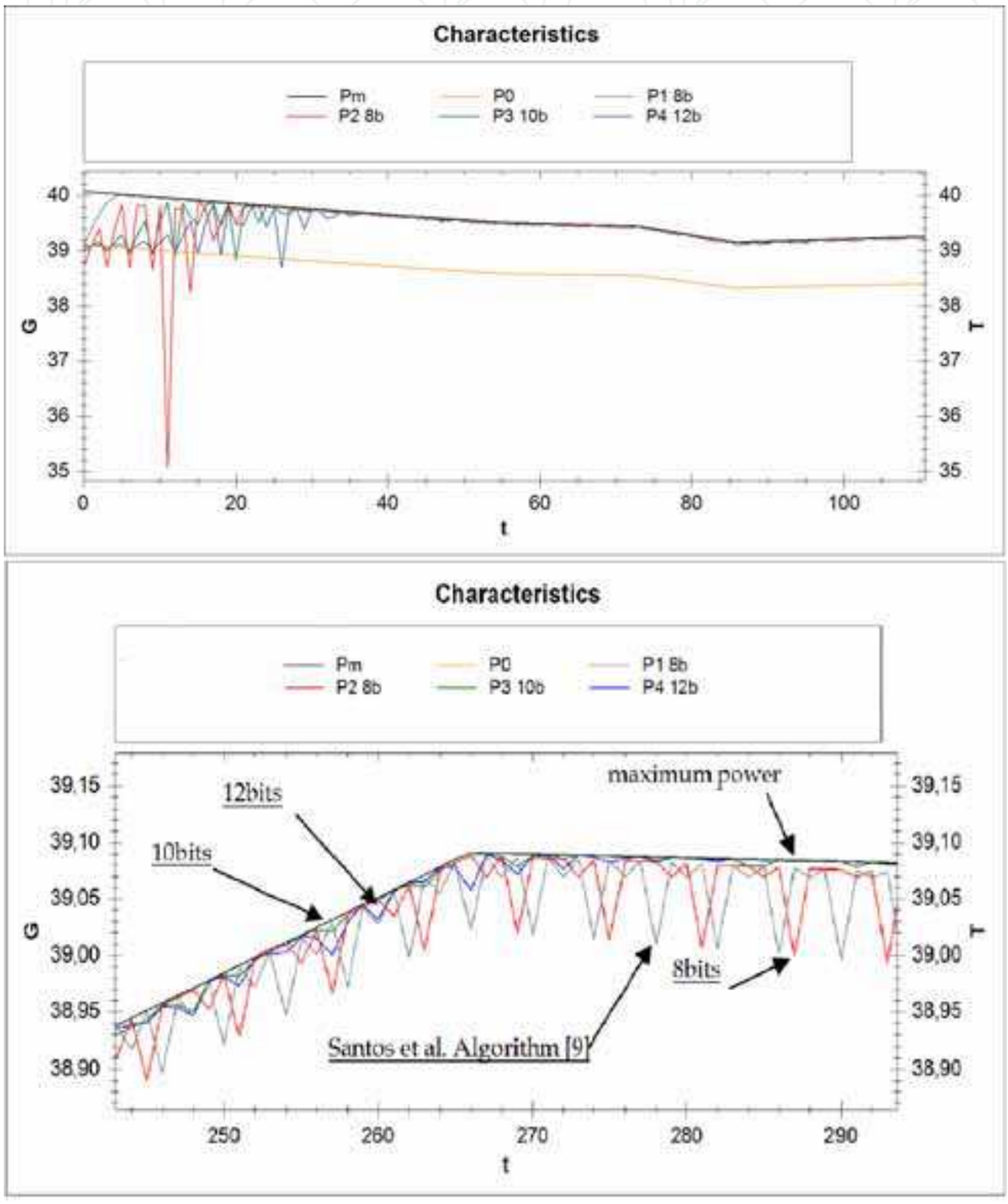

Fig. 18. The algorithm behavior: power output (a) and detail on power tracking (b)

The theoretical maximal power as seen in the figure is around 40 W. Our algorithm behaves best on 10 and 12 bits by staying as close as possible to the maximum power, while on 8 bits our algorithm's performance is still comparable to (Santos et al., 2006) algorithm.
Fig. 19. shows that the algorithm needs about 50 ms (less than 15 steps) to calibrate the variables D and Δ.

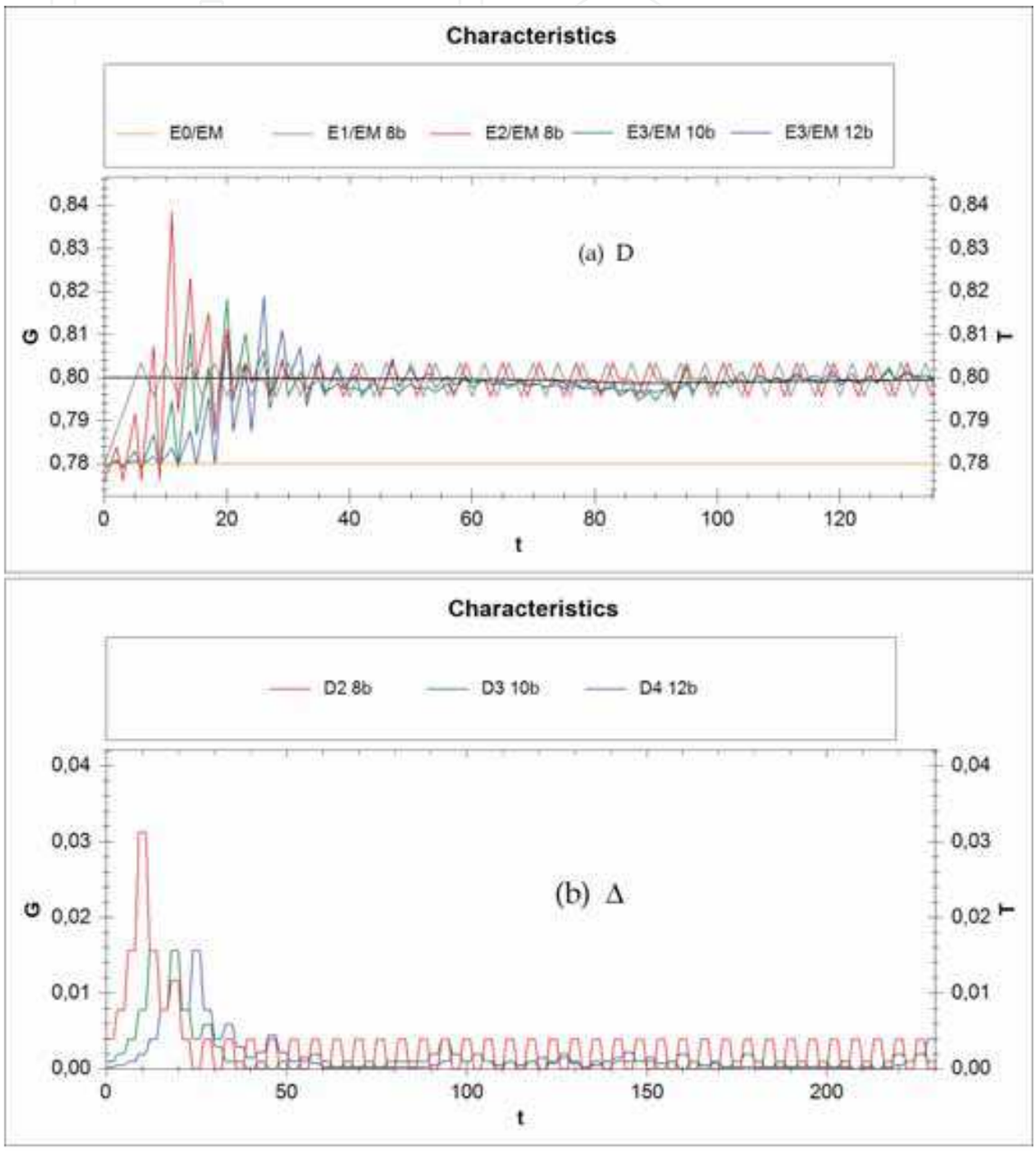

Fig. 19. The algorithm behavior: (a) D variation and (b) Δ variation

Using this algorithm we reached the following result, represented graphically:

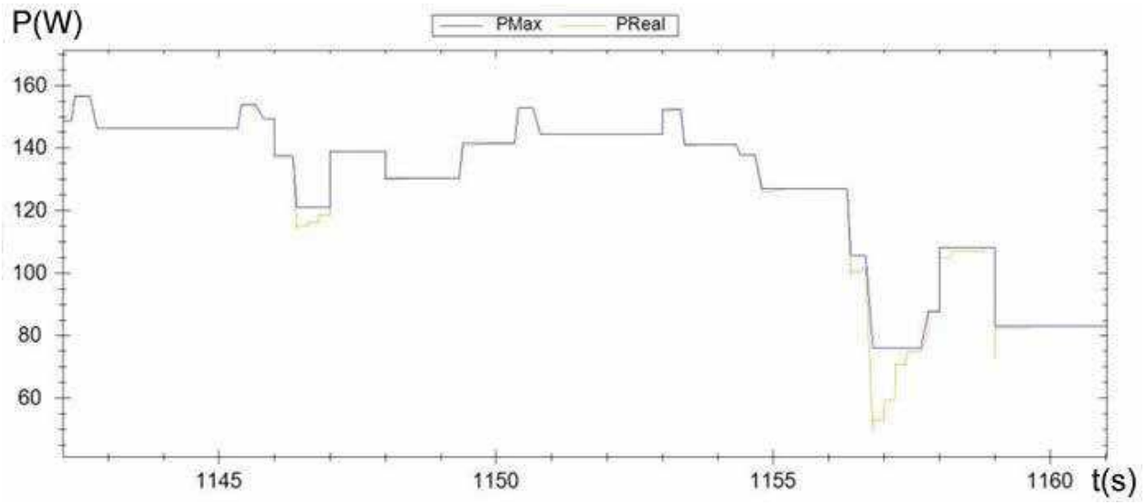

Fig. 20. Algorithm result for MPP's calculation with three points

Note that the power produced (P_{Real}) seeks the maximum power (P_{Max}) with a delay of *5* seconds. The algorithm needs 5 seconds to calibrate the variables Δ and d. The difference between the captured power and the available power is less than 5%.

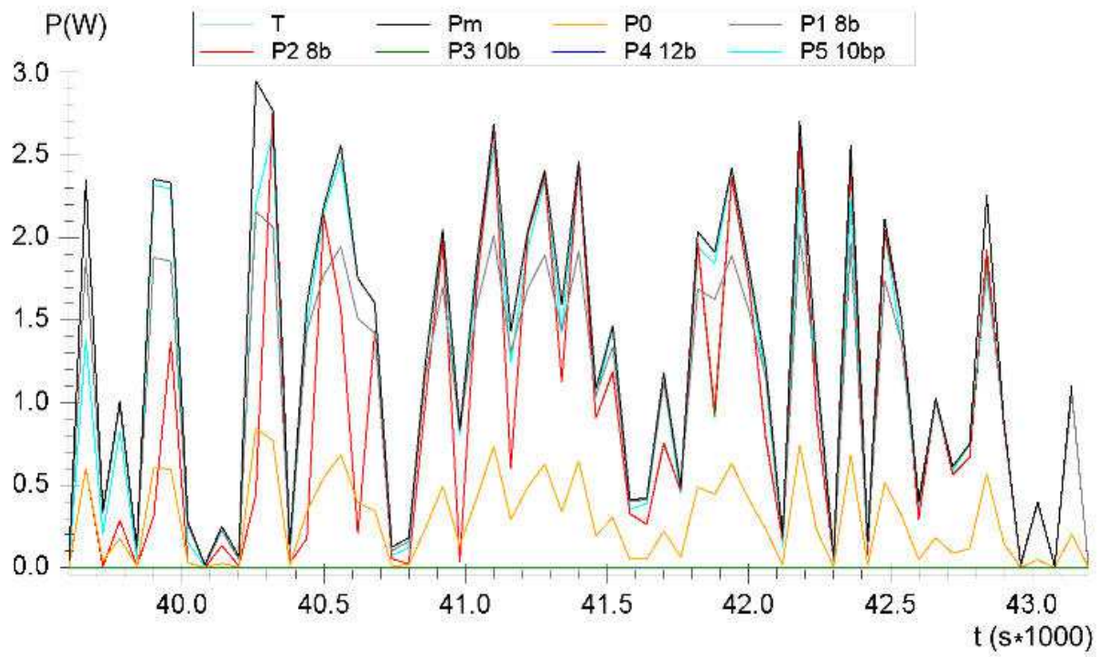

Fig. 21. Tracing of the maximum power through different algorithms, for high lightness and temperature variations

We made test implementations of this algorithm, on 8, 10 and 12 bits, and we compared their results with a set obtained from an 8 bits reference algorithm (P_{18b}) (Santos et al., 2006) and with one without MPPT (P_0), for very fluctuant meteorological conditions (simulated by our application - figure 5).

MPP determination using the reference algorithm (Santos 2007) is shown in Fig. 22.

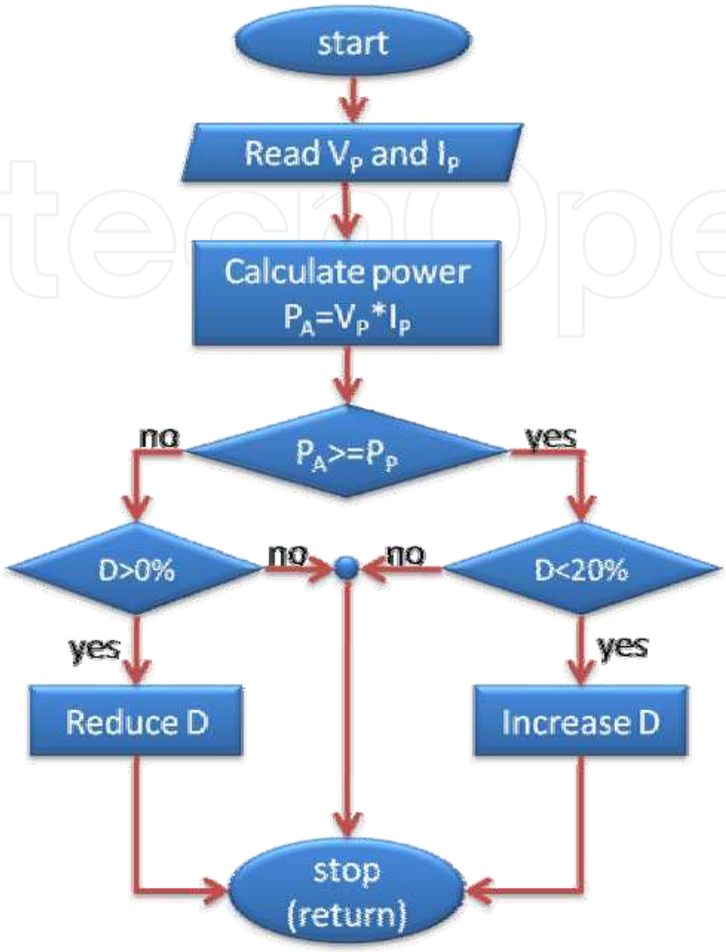

Fig. 22. J.L. Santos algorithm

7. Comparative determination between experimental and simulated results

To experimentally determine the advantages of MPPT chargers over the simple ones, we measured the output voltages and currents of these chargers, connected to two identical batteries, of *12V/80Ah*, and finally compared them with simulated results.

7.1 Experimental comparative determination between simple and MPPT charging

To measure load currents, we connected a resistor (R_l=*0.1Ω*) in series with each battery to the ground. Voltages on the resistors and on the battery-resistor assemblies were monitored for 16 hours with a four channel data aquisition device. To prevent the charge controllers to become out of service, following full charging of the batteries, we occasionally coupled load resistors at the battery terminals.

We realized the same measurements in two summer days: one predominant clear and a cloudy one.

We used the diagram below:

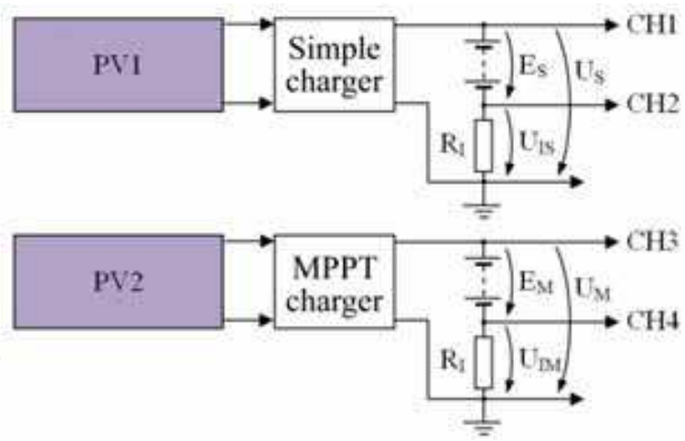

Fig. 23. The measurements diagram

The results are averaged over the hours shown in the tables below, together with calculated currents and powers. We also calculated the difference of power supplied by two regulators, *Pm-Ps*. The two powers and their difference were plotted in the figures below, and hourly average power data is presented in the table.

Ora	Us (V)	Uis (V)	Is (A)	Ps (W)	Um (V)	Uim (V)	Im (A)	Pm (W)	Pm-Ps (W)
4	11,92	0,05	0,50	5,96	11,97	0,07	0,70	8,38	2,42
5	11,93	0,13	1,30	15,51	12,09	0,17	1,70	20,55	5,04
6	12,12	0,20	2,00	24,24	12,33	0,25	2,50	30,83	6,59
7	12,33	0,28	2,80	34,52	12,35	0,35	3,50	43,23	8,70
8	12,47	0,33	3,30	41,15	12,53	0,40	4,00	50,12	8,97
9	12,70	0,39	3,90	49,53	12,69	0,47	4,70	59,64	10,11
10	13,04	0,42	4,20	54,77	12,90	0,49	4,90	63,21	8,44
11	13,13	0,42	4,20	55,15	13,04	0,48	4,80	62,59	7,45
12	12,98	0,44	4,40	57,11	12,91	0,51	5,10	65,84	8,73
13	12,90	0,38	3,80	49,02	12,86	0,44	4,40	56,58	7,56
14	12,80	0,33	3,30	42,24	13,01	0,39	3,90	50,74	8,50
15	12,63	0,29	2,90	36,63	13,10	0,33	3,30	43,23	6,60
16	12,60	0,20	2,00	25,20	13,14	0,24	2,40	31,54	6,34
17	12,57	0,13	1,30	16,34	12,87	0,15	1,50	19,31	2,96
18	12,36	0,05	0,50	6,18	12,61	0,07	0,70	8,83	2,65
19	12,30	0,01	0,10	1,23	12,49	0,01	0,10	1,25	0,02
20	12,26	0,00	0,00	0,00	12,32	0,00	0,00	0,00	0,00

Table 1. Electrical quantities measured and calculated for a clear day of summer

Energy provided by the two panels with associated chargers was determined as average hourly values and has daily values:

$$E_{S1} = 514,78Wh\ , \qquad E_{M1} = 615,86Wh \tag{22}$$

By using the MPPT charger, we get the following power gain:

$$A_1 = \frac{E_{M1}}{E_{S1}} = \frac{615,86}{514,78} = 1,1964 \tag{23}$$

So, in a bright summer day, tracking the MPP produced an energy surplus of 19.64%.

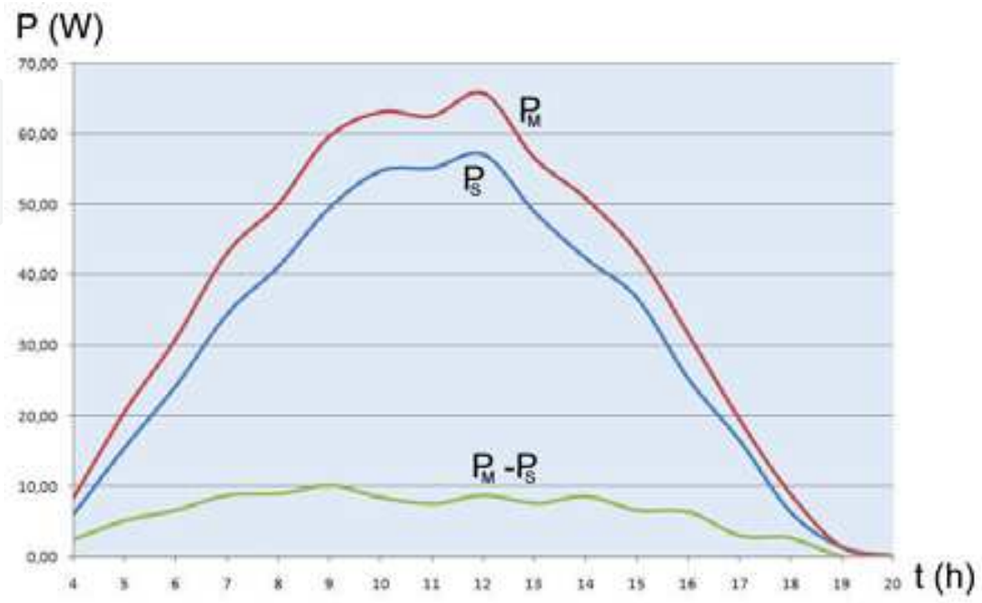

Fig. 24. Power transferred into batteries in a clear summer day

Ora	Us (V)	Uis (V)	Is (A)	Ps (W)	Um (V)	Uim (V)	Im (A)	Pm (W)	Pm-Ps (W)
4	11,90	0,03	0,30	3,57	11,93	0,03	0,30	3,58	0,01
5	11,86	0,06	0,60	7,12	11,99	0,07	0,70	8,39	1,28
6	12,00	0,08	0,80	9,60	12,18	0,10	1,00	12,18	2,58
7	12,14	0,09	0,90	10,93	12,12	0,12	1,20	14,54	3,62
8	12,27	0,13	1,30	15,95	12,29	0,16	1,60	19,66	3,71
9	12,47	0,16	1,60	19,95	12,42	0,20	2,00	24,84	4,89
10	12,76	0,14	1,40	17,86	12,58	0,17	1,70	21,39	3,52
11	12,89	0,18	1,80	23,20	12,78	0,22	2,20	28,12	4,91
12	12,71	0,17	1,70	21,61	12,61	0,21	2,10	26,48	4,87
13	12,64	0,12	1,20	15,17	12,57	0,15	1,50	18,86	3,69
14	12,61	0,14	1,40	17,65	12,80	0,18	1,80	23,04	5,39
15	12,46	0,12	1,20	14,95	12,91	0,14	1,40	18,07	3,12
16	12,49	0,09	0,90	11,24	13,01	0,11	1,10	14,31	3,07
17	12,49	0,05	0,50	6,25	12,78	0,06	0,60	7,67	1,42
18	12,34	0,03	0,30	3,70	12,57	0,03	0,30	3,77	0,07
19	12,30	0,01	0,10	1,23	12,49	0,01	0,10	1,25	0,02
20	12,27	0,01	0,10	1,23	12,33	0,01	0,10	1,23	0,01

Table 2. Electrical quantities measured and calculated for a cloudy summer day

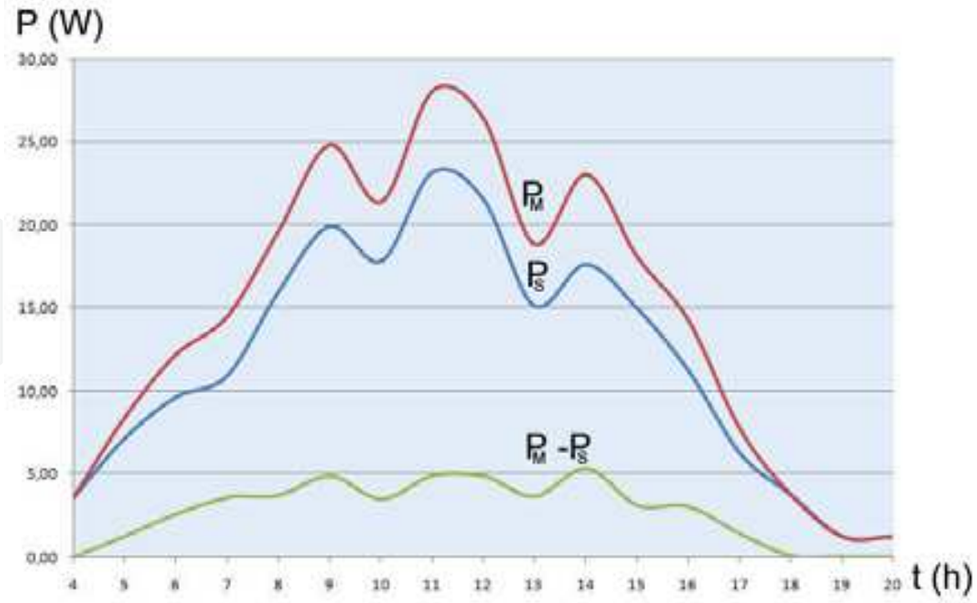

Fig. 25. The powers transferred to the batteries, in a cloudy summer day

The energy provided by the two panels during the cloudy day, via associated chargers, was computed based on average values of hourly and has daily values:

$$E_{S2} = 201,21Wh\,, \qquad E_{M2} = 247,38Wh \tag{24}$$

And the power gain caused by MPPT:

$$A_2 = \frac{E_{M2}}{E_{S2}} = \frac{201,21}{247,38} = 1,2295 \tag{25}$$

So, in a cloudy day of summer, using the MPPT charger, we obtain an energy surplus of 22.95%.

7.2 Experimental verification of the model and software

In parallel with the experimental determinations, we used the software application to estimate the energy increase caused by MPPT.

We modeled the $I(V)$ characteristic of the practically used panels, using the following parameters, which was able to produce a characteristic very similar with the one given by panel catalog:

a	R_P (Ω)	R_S (mΩ)	I_L (A)	I_0 (μA)	N_S	N_P
1,5	500	1	1,1	1,04	42	5

Table 3. Modelling parameters

Using this program we modeled the few specific experimental determinations made previously. For this evaluation we chose areas of interest $G \in \{100 \div 900\}\ W/m^2$ and $T \in \{20 \div 60\}\ ^0C$, sugested by the software.

The program window with the modelled *I(V)* characteristic is presented below:

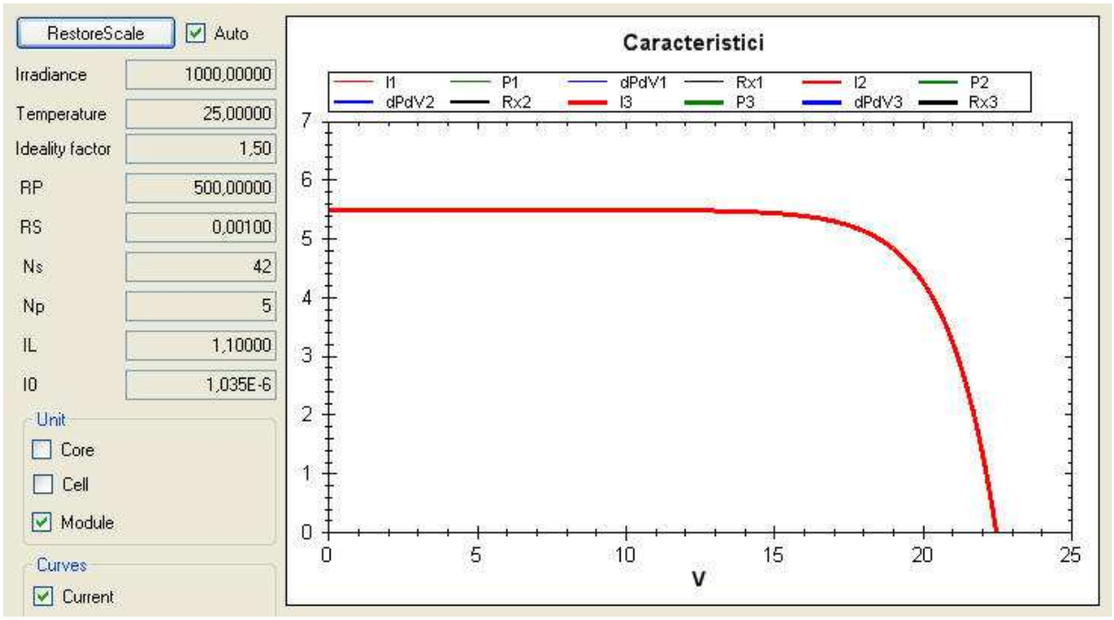

Fig. 26. The *I(V)* characteristic and model parameters of photovoltaic panel

P_{MPP} values are listed in the table below:

G \ T	**20**^{0}C	**30**^{0}C	**40**^{0}C	**50**^{0}C	**60**^{0}C
100 W/m^2	7,45	7,28	7,06	6,78	6,45
150 W/m^2	11,67	11,45	11,15	10,76	10,31
200 W/m^2	16,02	15,76	15,39	14,92	14,34
250 W/m^2	20,48	20,18	19,75	19,19	18,51
300 W/m^2	25,01	24,68	24,20	23,56	22,78
350 W/m^2	29,60	29,26	28,73	28,02	27,13
400 W/m^2	34,25	33,89	33,32	32,54	31,57
450 W/m^2	38,95	38,58	37,97	37,13	36,06
500 W/m^2	43,69	43,31	42,66	41,76	40,62
550 W/m^2	48,47	48,08	47,41	46,45	45,22
600 W/m^2	53,28	52,89	52,19	51,18	49,87
650 W/m^2	58,13	57,74	57,01	55,95	54,57
700 W/m^2	63,01	62,62	61,87	60,76	59,30
750 W/m^2	67,91	67,53	66,75	65,60	64,07
800 W/m^2	72,84	72,46	71,67	70,47	68,88
850 W/m^2	77,79	77,42	76,62	75,38	73,72
900 W/m^2	82,77	82,41	81,59	80,31	78,58

Table 4. The MPP power under different weather conditions

In this table we have marked with a gray background the P_{MPP} values which are representative for the times of day in which experimental measurements were made.

For G and T values in the table above, we determined the appropriate powers for direct connection of panel to the battery, P_S, from $P(V)$ characteristics, as shown graphically below.

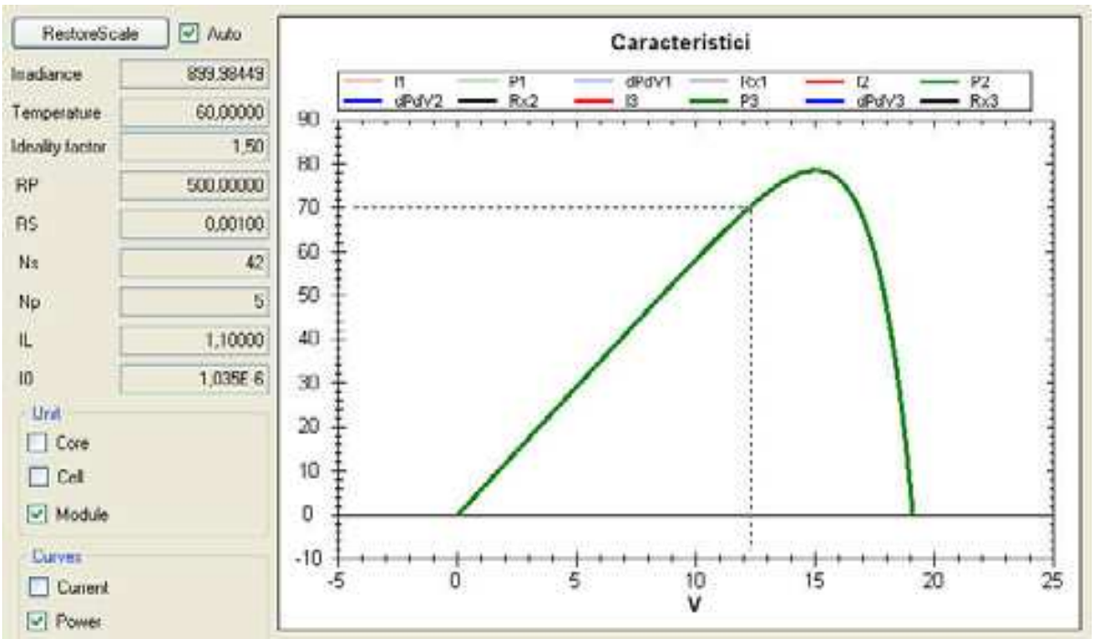

Fig. 27. The $P(V)$ characteristic of the panel model, at $T=60^0C$ and $G=900W/m^2$

The determined values (P_S), together with those of MPP (P_{MPP}), are listed in the table bellow:

G (W/m²)	**T** (⁰C)	**P_{MPP} (W)**	**P_S (W)**	**P_{MPP}/ P_S**
100	20	7,45	6	1,2417
300	30	24,68	20	1,2340
500	40	42,66	36	1,1850
700	50	60,76	52	1,1685
900	60	78,58	71	1,1226

Table 5. MPP power, direct power and power gain, in different weather conditions

From this table we see that in most cases, power ratio is similar to situations experimentally determined, with errors under *1%*, correspondent to average illuminations of $500W/m^2$ (sunny day), respectively $300W/m^2$ (cloudy day).

8. Conclusions

A general approach on modeling photovoltaic modules is presented. The proposed MPP tracking computational method is based on a DC/DC converter control with an original algorithm. The theoretical evaluations of the MPPT advantages, based on the proposed model, sugest that the power gain, obtained by MPP tracking, is higher than 27%.
We developed, simulated and evaluated two MPPT algorithms, based on presented model. The proposed algorithms are independent of the used solar panel type, which could be considered a "black box".

The algorithms starts from the known fact that the power curve at given conditions have a global maximum. This algorithm is useful for any kind of electrical energy source, where this condition is covered. The performance of the algorithm is limited by the precision of measurement blocks and by the word size of used microcontroller.
Algorithm has relatively short response times, covering the difference between the extracted power and MPP in less than 15 steps (~ 50ms). These results are very good compared with some widely-adopted MPPT algorithms (Faranda et al., 2007). The power loss depends on the working frequency of the control module.
We made some experimental measurements on an implemented MPPT charging circuit and a simple one. The resulted MPPT power gain was lower with about 7% than the theoreticaly one, due to different efficiency of the charging circuits. The experimental results were compared with the simulated ones, for the same conditions and panel parameters. This comparison reveals that the differences between experimental data and simulated characteristics were less than *1%*.
We intend to tune and develop the presented method to improve the response time and efficiency and to apply it to other kind of unconventional energy sources.

9. Acknowledgement

The presented research work was done within the SINERG project (PNCDI2 22-140/2008), funded by the Romanian National Center for Programs Management.

10. References

Chenni, R.; Makhlouf, M.; Kerbache, T.; Bouzid, A. (2007). A detailed modeling method for photovoltaic cells, *Energy*, Vol. 32, no 9, 2007, pp. 1724-1730, ISSN 0360-5442

Faranda, R.; Leva, S.; Maugeri, V. (2007). Comparative study of ten Maximum Power Point Tracking algorithms for Photovoltaic System, *U.P.B. Scientific Bulletin*, Series C, Vol. 69, No. 4, 2007, pp. 271-278, ISSN 1454-234x

Hui, J. (2008). *An Adaptive Control Algorithm for Maximum Power Point Tracking for Wind Energy Conversion Systems - MSc thesis*, Queen's University Kingston, December 2008, Ontario, Canada

Milea, L.; Franti, E.; Dragulinescu, M.; Oltu, O.; Dascalu, M. (2008). Residential photovoltaic energetic system, optimized with an FPGA based control unit, *Proceedings of The 3rd International Conference on ENERGY & ENVIRONMENT (EE'08)*, pp. 518-522, ISBN: 978-960-6766-43-5, February 2008, WSEAS, Cambridge

Milea, L.; (2010). *Sources, Systems and Circuits for Unconventional Energies - PhD Thesis*, University POLITEHNICA of Bucharest, March 2010, Bucharest, Romania

Santos, J.L.; Antunes, F.; Chehab, A.; Cruz, C. (2006). A maximum power point tracker for PV systems using a high performance boost converter, *Solar Energy*, Vol. 80, Issue 7, July 2006, pp. 772–778, ISSN: 0038-092X

Yang, H.; Zhou, W.; Lu, L.; Fang, Z. (2008). Optimal sizing method for stand-alone hybrid solar–wind system with LPSP technology by using genetic algorithm, *Solar Energy*, Vol. 82, Issue 4, April 2008, Pages 354-367, ISSN: 0038-092X

Zafiu, A.; Ionescu, V.; Bizon, N.; Ghita, C.; Oproescu, M. (2009). A detailed model for PV Simulation and MPP Tracking with three points, *Proceedings of the International Conference on ELECTRONICS, COMPUTERS and ARTIFICIAL INTELLIGENCE – ECAI' 09*, ISSN – 1843 – 2115, July 2009, Pitesti, Romania

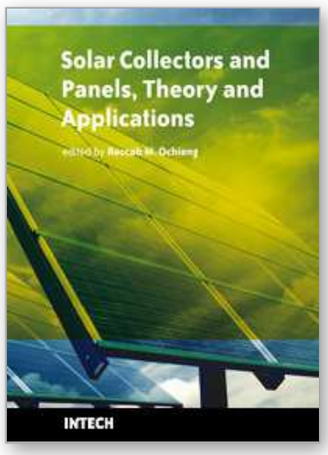

Solar Collectors and Panels, Theory and Applications

Edited by Dr. Reccab Manyala

ISBN 978-953-307-142-8

Hard cover, 444 pages

Publisher Sciyo

Published online 05, October, 2010

Published in print edition October, 2010

This book provides a quick read for experts, researchers as well as novices in the field of solar collectors and panels research, technology, applications, theory and trends in research. It covers the use of solar panels applications in detail, ranging from lighting to use in solar vehicles.

How to reference

In order to correctly reference this scholarly work, feel free to copy and paste the following:

Lucian Milea, Adrian Zafiu, Orest Oltu and Monica Dascalu (2010). Theory, Algorithms and Applications for Solar Panel MPP Tracking, Solar Collectors and Panels, Theory and Applications, Dr. Reccab Manyala (Ed.), ISBN: 978-953-307-142-8, InTech, Available from: http://www.intechopen.com/books/solar-collectors-and-panels--theory-and-applications/theory-algorithms-and-applications-for-solar-panel-mpp-tracking

INTECH
open science | open minds

InTech Europe
University Campus STeP Ri
Slavka Krautzeka 83/A
51000 Rijeka, Croatia
Phone: +385 (51) 770 447
Fax: +385 (51) 686 166
www.intechopen.com

InTech China
Unit 405, Office Block, Hotel Equatorial Shanghai
No.65, Yan An Road (West), Shanghai, 200040, China
中国上海市延安西路65号上海国际贵都大饭店办公楼405单元
Phone: +86-21-62489820
Fax: +86-21-62489821

IntechOpen